

Experimental Evidence of Low Impurity Transport in NSTX

D. Stutman^a, M. Finkenthal^a, C. Bourdelle^b, E. Synakowski^b, J. Menard^b, D. Darrow^b,
B. Leblanc^b, R. Bell^b, V. Soukhanovskii^b, M. Gilmore^c, S. Kaye^b

^a*Johns Hopkins University, Baltimore, MD 21218, USA*

^b*Princeton Plasma Physics Laboratory, Princeton University, Princeton, NJ 08543, USA.*

^c*University of California, Los Angeles, CA 90095, USA*

Introduction

The Spherical Torus (ST) concept is presently explored in experiments at the 1 MA current level, as an alternative path to economical fusion energy [1]. One of the main improvements predicted to occur in a ST is a reduced level of electrostatic microturbulence. The reduction is partly due to the low aspect-ratio geometry and partly to the high beta [2,3]. Also, due to the low magnetic field, strong field gradient and high beta, the ExB flow shear is predicted to be more effective in suppressing long wavelength turbulence [2]. Indeed, the first thermal transport studies performed on the National Spherical Torus Experiment (NSTX) suggest that the ion thermal transport is close to neoclassical. At the same time, the analysis of these data has revealed puzzles pertaining to the origins of the ion heating and the partitioning of the heat flow between ions and electrons [4].

Here we report on the first perturbative transport experiments meant to characterize the particle impurity transport in the high beta ST plasma. This technique of assessing the local transport characteristics obviates any uncertainties in the power balance analysis, thereby yielding an unambiguous probe of a single transport channel. Non H-mode discharges auxiliary heated with 1.5 MW of neutral beam power have been investigated so far.

Experiment

The experiments consisted in injecting brief (≈ 20 ms), non-perturbing ($n_{\text{neon}}/n_e \approx 0.5\%$) puffs of neon during the current flat top of MHD quiescent ($q(0) > 1$) discharges and measuring its penetration with two Ultrasoft X-ray (USXR) diode arrays [5]. We chose neon because of its strong signature in the USXR range and because previous experiments show that low-Z impurity transport is often correlated with the thermal transport of the working ions [6]. The discharges here analyzed had major/minor radius $R/a \approx 0.85$ m/0.65 m, 0.8 MA current, 4.5 kG toroidal field, 0.8 keV and $3 \cdot 10^{13}$ cm⁻³ central electron temperature and density, respectively.

At ionization equilibrium the dominant Ne charge states in the above plasma would be fully stripped Ne¹⁰⁺ for $\approx r/a \leq 0.5$ and He-, H-like Ne^{8,9+} for $\approx 0.5 \leq r/a \leq 0.9$. Since the Ne^{8,9+} ions emit mainly resonance lines between 0.9-1.0 keV, whereas the Ne¹⁰⁺ ions mainly recombination continuum above ≈ 1.4 keV, we separately measured their spatial distribution

by simultaneously filtering the upper and lower diode arrays with Be foils having 0.6 keV and 1.4 keV cutoff energy, respectively (Fig. 1). In addition, the USXR and VUV spectral lines from peripheral and core Ne ions were recorded by time resolved, high resolution spectrometers.

The USXR emissivity is obtained by the inversion technique detailed in [7]. The neon contribution is determined by subtracting the background from consecutive reproducible discharges. The puff does not perturb any of the plasma profiles, the only measurable effects being an increase in the USXR emission and a transient increase in the peripheral radiated power of less than $\approx 0.01 \text{ W/cm}^3$.

The evolution of the Ne emissivity in the above energy ranges is shown in Fig. 2. The emission from $\text{Ne}^{8,9+}$ ions forms a hollow shell, which stagnates at mid-radius until a MHD event occurs at $t \approx 260 \text{ ms}$. During the same interval almost no increase in the core emission above 1.4 keV is observed, indicating that the fully ionized Ne is also absent in that region. In conclusion, the injected neon quickly penetrates to about $r/a \approx 0.6-0.7$, where then stagnates for the duration of the MHD quiescent phase. At the reconnection event the shell of $\text{Ne}^{8,9+}$ ions collapses into the core, where it is ionized to Ne^{10+} within a few ms. This gives rise to the strong burst of $E > 1.4 \text{ keV}$ emission seen in Fig. 2 after 260 ms.

Modeling

The above evolution has been modeled using a time-dependent version of the computational package described in [7]. Briefly, line and continuum radiative coefficients are first computed for each neon charge state and filter. USXR emissivity profiles are then computed using these coefficients and the Multi-Point Thomson Scattering n_e and T_e profiles. Finally, the evolution of these profile in the two energy ranges is simultaneously fitted by varying the diffusive (D) and convective (V) transport coefficients in the MIST impurity transport code [8]. For simplicity we assumed two distinct transport regions, each characterized by a constant diffusion coefficient and a convective velocity linear in the radial coordinate. The high-resolution spectra together with the bolometric profiles serve to constrain the evolution of the peripheral Ne source, as well as the fractions of He- and H-like Ne ions.

The transport solution reproducing the Ne emission history in Fig. 2 is shown in Fig. 3a. The fit obtains with diffusive transport, having D of a fraction of a square meter per second inside $r/a < 0.6$ and rapidly raising to a few m^2/s outside this radius. The diffusive character of impurity transport in NSTX has been better ascertained in recent experiments, in which a fast varying Ne source could be produced. (See [9] on the role of a fast varying perturbation in separating the diffusive and convective contributions). The estimated error in our result is a few tens of percent in the outer plasma and larger in the central region, where little neon penetrates.

The intrinsic carbon profile also indicates a transport discontinuity around $r/a \approx 0.6-0.7$. Similar modeling of the background USXR emission in these discharges reveals a ‘bulge’ in the C density at this radius [7]. Although D and V cannot be separately estimated

from the steady-state analysis, the particle flux consistent with this ‘bulge’ shows a rapid decrease at $r/a \approx 0.6-0.7$.

The significance of the above results can be seen by comparison with the predictions of the neo-classical (collisional) theory. Overlaid with the experimental estimate in Fig. 3a is the diffusion coefficient computed with the NCLASS code [10]. The comparison indicates that inside $r/a \approx 0.6$ the particle diffusion approaches the collisional limit. This in turn would imply that, even in non H-mode discharges, the level of turbulent ion transport is NSTX low. As earlier mentioned, a similar conclusion obtains from the preliminary assessment of ion thermal diffusivity [4].

A recent microstability analysis of the above discharges suggests that the reduced level of anomalous ion transport is an intrinsic property of the beam heated NSTX plasmas [11]. Fig. 3b illustrates this prediction, showing that the low $k_{\theta}\rho_i$ modes believed responsible for ion turbulent transport in tokamaks (ITG and TEM) are essentially stable inside $r/a \leq 0.6$. Outside this radius they grow unstable, while at the same time the $E \times B$ shearing rate decreases. In conclusion, the existence of a region of near neoclassical diffusion inside $r/a < 0.6-0.7$, bounded by a region of higher transport as depicted in Fig. 3a, appears qualitatively consistent with the microstability predictions.

In addition, recent perturbative transport scaling experiments indicate a steady decrease in the peripheral neon penetration with increasing magnetic field, suggesting a finite Larmor radius effect on ion transport. This inference is also supported by microwave reflectometer measurements of the correlation length of peripheral density fluctuations, which show a strong decrease in the ion turbulence scale with increasing magnetic field.

At the same time, the global confinement (which consistently exceeds the conventional tokamak scaling) does not change with the magnetic field. Since the ion channel appears to change, this would suggest that the electron transport strongly dominates in NSTX, which is consistent with the initial thermal diffusivity estimates [4]. The large $k_{\theta}\rho_i$, Electron Temperature Gradient modes are predicted to be unstable in these plasmas and may play a role in this respect [11]. In conclusion, the initial NSTX observations hint at a different transport picture in a ST compared to conventional tokamaks.

Work supported by U.S. DOE Grant No. DE-FG02-99ER54523 at Johns Hopkins University

References

1. Y. -K. Peng, Phys. Plasmas **8**, 1681(2000)
2. M. Kotschenreuther *et al.*, Nuclear Fusion **40**, 677(2000)
3. G. Rewoldt *et al.*, Phys. Plasmas **3**, 1667(1996)
4. E. Synakowski *et al.*, Proceedings of the Transport Barrier and H-mode Workshop, Toki, Japan, 2001
5. D. Stutman *et al.*, Rev. Sci. Instrum. **70**, 572 (1999)
6. E. Synakowski *et al.*, Phys. Fluids **B**, (2215) 1993
7. D. Stutman *et al.*, Proc. 28th Euro. Conf. on Plasma Physics and Contr. Fusion, Madeira, Portugal, 2001
8. R.A. Hulse, Nuclear Technology/Science **3**, 259 (1983)
9. N. J. Lopez Cardozo, Plasma Phys. Control. Fusion **37**, 799 (1995)
10. M. R. Wade, W. A. Houlberg and L.R. Baylor, Phys. Rev. Lett. **84**, 282(2000)
11. C. Bourdelle *et al.*, submitted to Nuclear Fusion

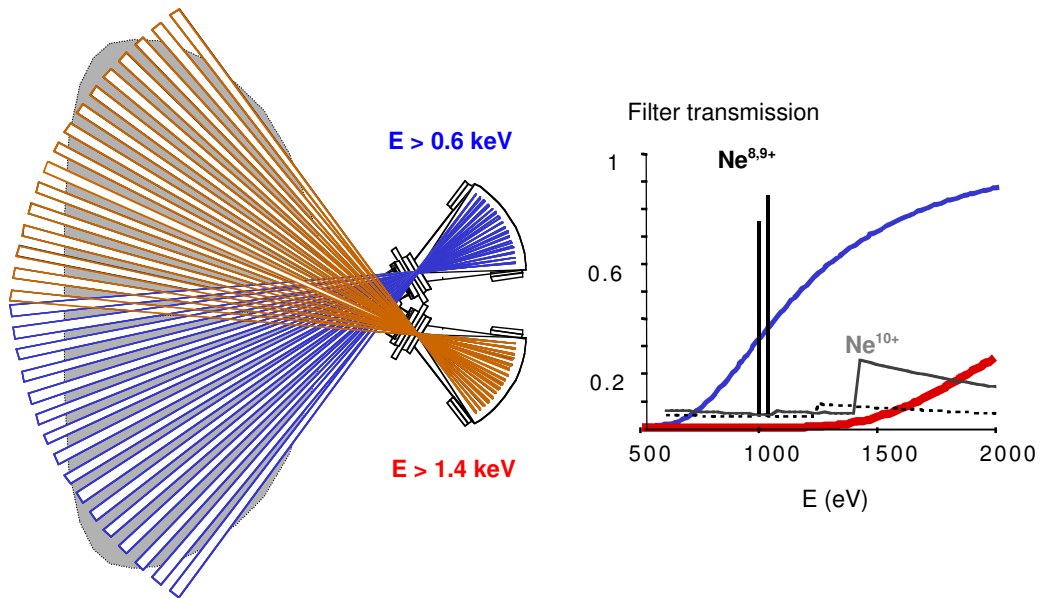


Figure 1. Setup of the USXR system for the Ne injection experiments

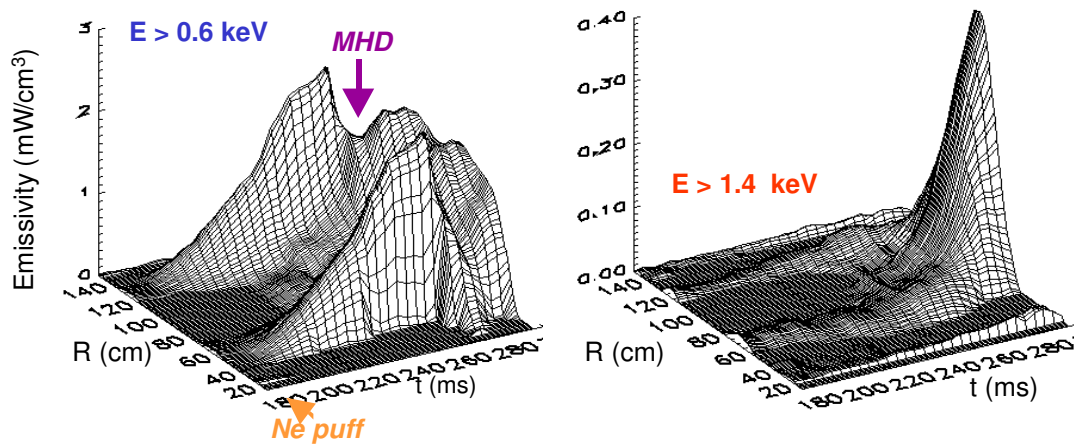


Figure 2. Evolution of the Ne emissivity in the $E > 0.6$ keV and $E > 1.4$ keV spectral ranges

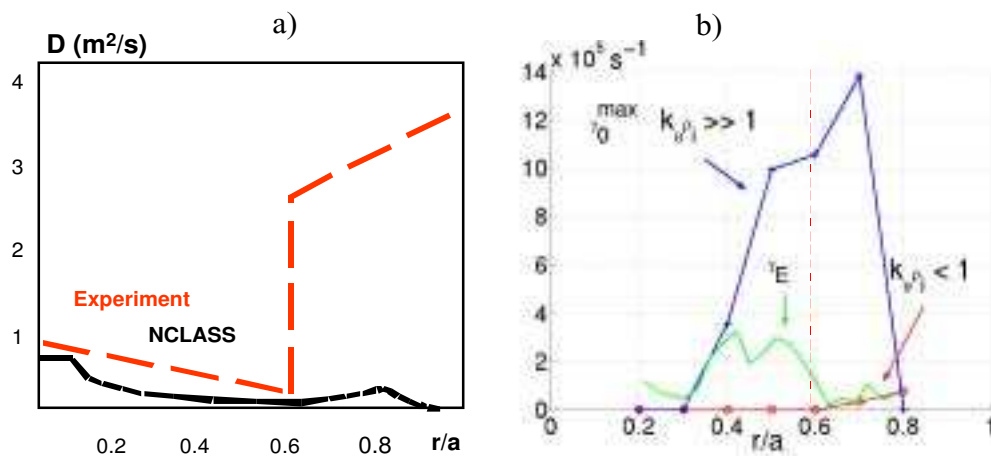


Figure 3. a) Best-fit transport solution and neoclassical diffusion calculated by NCLASS
 b) Growth rates of most unstable drift modes and NCLASS $\mathbf{E} \times \mathbf{B}$ shearing rate [11]